Functional Materials 17, No.2 (2010)

Interface properties of Bi-contained iron garnet films/GGG-substrates

V.N.Berzhansky, A.V.Karavainikov, E.T.Milyukova, A.R.Prokopov, A.N.Shaposhnikov

V.Vernadsky Taurida National University, 4 Acad. Vernadsky Ave., 95007 Simferopol, Ukraine

Received November 11, 2009

The concentration dependences of garnet-constituting elements, magneto-optical properties and surface morphology of $(BiSmLu)_3(FeGaAl)_5O_{12}$ LPE iron garnet films / (111) $Gd_3Ga_5O_{12}$ substrate interfaces have been studied. The magnetic properties and complex shapes of magneto-optical hysteresis loops for some garnet films have been found to depend on the film/substrate-interface characteristics. In some films, the effect of the sublattice magnetic moment spin-reorientation accompanied by the subsequent thermo-magnetic hysteresis has been revealed near the compensation point.

Исследованы концентрационные зависимости гранатообразующих элементов, магнитные свойства и морфология поверхности интерфейса Bi-содержащих монокристаллических пленок ферритов-гранатов состава $(BiSmLu)_3(FeGaAl)_5O_{12}$ — подложка ГГГ ориентации (111). Показано, что магнитные свойства и сложные формы магнитооптических петель гистерезиса исследованных пленок могут определяться свойствами интерфейса пленка-подложка. В некоторых пленках вблизи температуры компенсации обнаружен эффект "опрокидывания" магнитного момента подрешеток, сопровождающийся последующим температурным магнитным гистерезисом.

1. Introduction

As is well known, the initial and the final stages of liquid phase epitaxy (LPE) are nonstationary processes, so the film/substrate and film/air transient layers may be formed at those stages [1–3]. Those layers may influence the properties of the film as a whole [4–6]. In [7], we have investigated the thickness dependences of magnetic properties for $(BiSmLu)_3(FeGaAl)_5O_{12}$ LPE iron garnet films being used for thermo-magnetic data recording. Usually, such films grow under the high supercooling values ΔT_s, so the composition of growing films is extremely sensitive to the growth conditions and the stability thereof. It has been shown that during the film growth process, the layers with different H_c, Θ_F, T_c, and $T_{comp.}$ values are formed in the films along the growth axis. The aim of this work is to study the concentration of the garnet-constituting elements in the $(BiSmLu)_3(FeGaAl)_5O_{12}$ LPE iron garnet films/ (111) $Gd_3Ga_5O_{12}$ (GGG) substrates interfaces and effect of concentration on morphology and magnetic properties of the films.

2. Experimental

$(BiSmLu)_3(FeGaAl)_5O_{12}$ LPE iron garnet films of 3–6 μm thickness were grown on the GGG (111) single crystal substrates from a supersaturated solution-melt based on $PbO–B_2O_3–Bi_2O_3$ flux. The as-grown and polished films were etched step by step using Ar^+ ions to the film thickness less than 2 μm. Then the films were etched using an unfocused ion beam to form a "wedge" of 10–12 mm length with the thickness varying from 1.5–1.7 μm to zero.

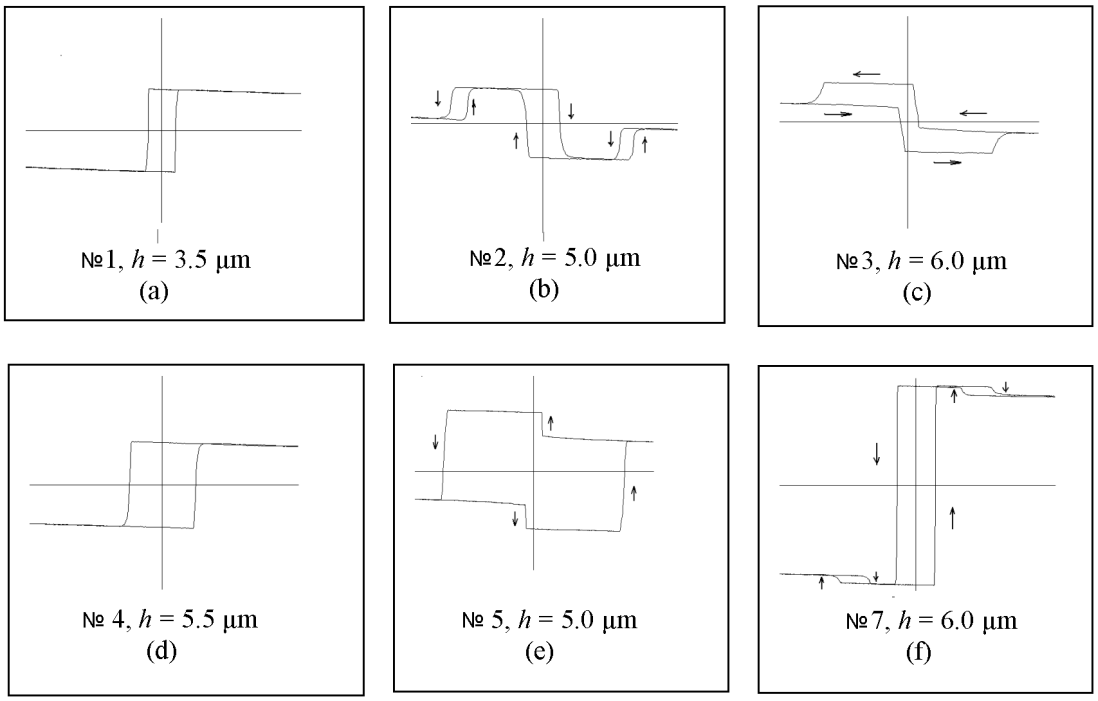

Fig. 1. Faraday hysteresis loops of as-grown films we investigated. T = 25°C. H_{max} = 2 kOe, Θ_{Fmax} = 2.2°.

The following film characteristics were measured after each etching step and then along the wedge (i.e. along the film thickness change):

— the film elemental composition and surface state by electron microprobe microanalysis (EPMA) and scanning electron microscopy (SEM);

— magneto-optical hysteresis loops (wherefrom H_c, Θ_F, T_c, $T_{comp.}$ were determined) using a Faraday magneto-polarimeter at λ = 655 nm and T = 10–80°C and lattice mismatch Δa- by X-ray diffractometer (XRD).

3. Results and discussion

The Faraday hysteresis loops (FHLs) of as-grown films at T = 25°C [7] are shown in Fig. 1. To measure the interface properties, chosen were the Samples 2, 5, 7 with complex loop shapes but being monolayer according to XRD, as well as the Sample 3 with complex FHL and Sample 4 with usual FHL (both bilayer according to XRD).

The FHL measurements of Sample 4 have shown double inversion of Θ_F sign (Fig. 2a) and $T_{comp.}$ variation (Fig. 2b) along the wedge. Three thickness regions are observable along the wedge: the film/air interface region 1 ($1.3 \le h \le 1.7$ μm) with "right" FHLs; central region 2 ($0.7 \le h \le 1.3$ μm) with "left" FHLs and film/substrate interface region 3 ($h \le 0.7$ μm) with "right" FHLs. In these regions, $T_{comp.}$ increases from region 1 to region 2 from 15 up to 24°C, and decreases from region 2 to region 3 from 24 down to 21.5°C. Such a behavior of Θ_F and $T_{comp.}$ may be due only to chemical composition changes along the film thickness. So, Fig. 2c shows the concentration depth profile and FHLs along the wedge (i.e. along the film thickness change) in the regions 1–3 of the Sample 4 at the film thickness below 1.8 μm (T = 22°C, H_{max} = 2 kOe). It is seen that in the film volume and at the film/substrate interface, there is a concentration gradient of garnet-constituting elements. In the region 2, the total concentration of Ga^{3+} and Al^{3+} ions is higher than in region 1 and the transient film-substrate region 3 is enriched in substrate elements Gd^{3+} and Ga^{3+}. As is well known [8], the Ga^{3+} and Al^{3+} concentration increase in tetrahedral positions in garnet causes increased $T_{comp.}$ and decreased T_c. Thus, the increase of the total Ga^{3+} and Al^{3+} concentration from 1.2 to 1.6 at./f.u. (atoms per formula unit) results in increased $T_{comp.}$ in the region 1 as compared to region 2. In region 3, the amount of Ga^{3+} and Al^{3+} exceeds 2.5 at./f.u., but Θ_F is positive and $T_{comp.}$ value is lower than in region 2. We have assumed that this is due to low depth reso-

lution of EPMA-method (deep penetration of electron beam); really, the main amount of Ga^{3+} as analyzed by EPMA is in substrate but not in the film.

Note that FHL in region 1 at 22°C would have to be a superposition of hysteresis loops of opposite signs from the inner layers and to have more complex shape. However, it is possible that the proximity of $T_{comp.}$ to the measuring temperature causes reorientation of the magnetic moments in the second layer due to strong exchange molecular field of the near-surface layer. Thus, we observe the synphase re-magnetization process in all the layers and the simple FHL shape in region 1 at 22°C. But at T = 12°C, we observe a complex FHL (see inset in Fig. 2c). Its characteristic feature is the Θ_F sign change when the magnetization field decreases.

In the region 2 of the Sample 4 at $T \le T_{comp.}$ (region of the "left" FHLs), the film magnetization in the field $H \ge 3$ kOe led to an abrupt change of the Θ_F sign at a certain field H_f, i.e. to "turnover" of the sublattice magnetic moment. These high-field state was" frozen" and persisted at the field decrease and the subsequent reversal. In that case, FHLs from the "left" became "right". The return to the low-field phase and the original FHLs appearance occurred only after lowering the temperature to $T \le T_{comp.}$, i.e. we observed the temperature magnetic hysteresis. The field H_f causing that effect was lowered when T approaches $T_{comp.}$:at T = 23°C, H_f = 3.7 kOe, at T = 23.5°C, H_f = 1.5 kOe. This effect could be explained as follows. The phase transition of "compensation point" type in three-sublattices ferrimagnets is due to competition of paramagnetic rare-earth ions magnetized in the exchange field with iron ions in a- and d-sublattices, or due to competition of iron ions in a- and d-sublattices. In the films we investigated, the second phase transition case is realized, because Sm-ferrite-garnet has no compensation point of the magnetic moment [9]. The investigated films exhibit a large magnetic uniaxial anisotropy (over 15 kOe). Therefore, accordingly to the field-temperature H–T phase diagram [10], at the film magnetization along the easy axis and approaching to $T_{comp.}$, different types of collinear and noncollinear phases may exist in the films. The collinear phases have different magnetic moment orientations in iron sublattices with respect to the external magnetic field. At $T < T_{comp.}$, the octahedral iron sublattice is oriented along the

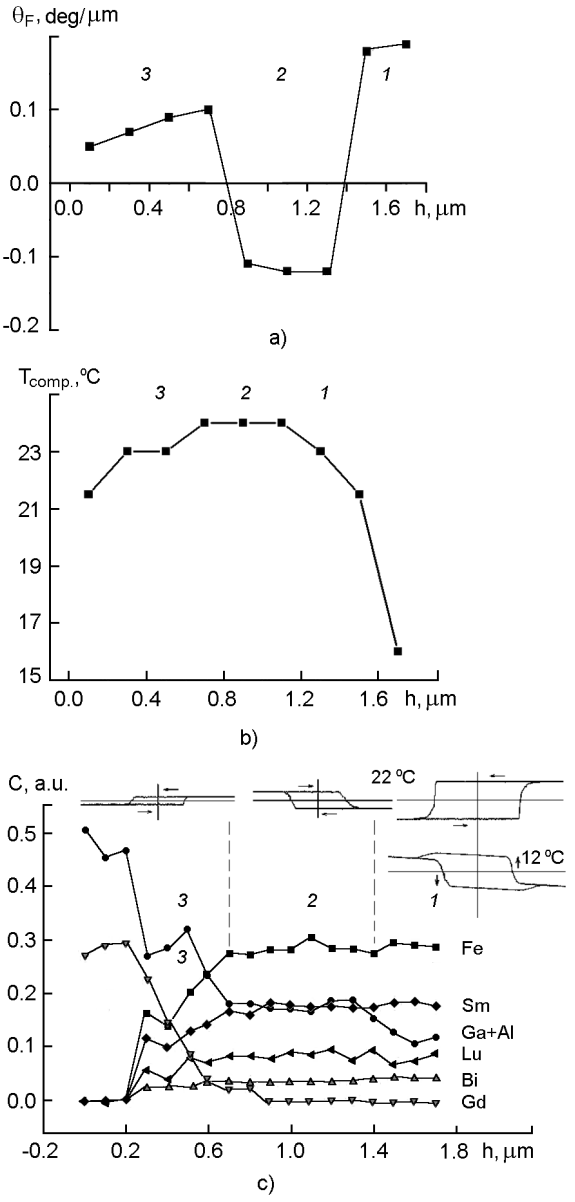

Fig. 2. $\Theta_F(h)$ at T = 22°C and H_{max} = 2 kOe (a); $T_{comp.}(h)$ (b); concentration depth profile and FHLs (c) along the wedge of the sample 4.

field, the re-magnetization process causes the "left" FHL. At $T > T_{comp.}$, the tetrahedral iron sublattice is oriented along the external magnetic field and the re-magnetization process results in the "right" FHL. A sharp "turnover" of the sublattice magnetic moments in certain magnetizing fields we observed is associated with the transition between the collinear phases, which is a jump-type first order phase transition. In accordance to the H–T diagram, the field of this transition should decrease when approaching the compensation point, which is observed in experiment really. In addition,

the observed temperature magnetic hysteresis also confirms that a first order phase transition occurs really in the system.

Fig. 3 shows the distribution of elements along the wedge and FHLs at $T = 22°C$ in the Sample 5. The initial sample had the complex FHL shape, this shape persisted until the substrate itself, and FHL became simple "left" only near the interface. The total content of Ga^{3+} and Al^{3+} near the substrate exceeded 2 at./f.u. With increasing h, Ga^{3+} content decreased, Θ_F changed its sign, and FHL acquired a shape typical of a film with a variable composition across the thickness, where the layers have $T_{comp.}$ values above and below the measurement temperature, thus resulting in a complex FHLs shapes.

In the Sample 7, as in the Sample 5, the FHLs near the film/substrate interface are "left", the total Ga^{3+} and Al^{3+} content in this region reached 1.5 at./f.u., $T_{comp.} = 35°C$. With increasing h, Ga^{3+} content decreased, Θ_F changed its sign, and FHL acquired a shape typical of a film with a variable composition across the thickness.

As is seen from Fig. 1, FHLs of the Samples 3, 5 and 7 differ from each other, but FHLs of transition film/substrate layers therein are identical. As to magnetic state, these samples are at least double-layer. In these samples, a layer with a low concentration of diamagnetic ions and the "right" FHL grows on a layer with a high concentration of diamagnetic Ga^{3+} and Al^{3+} ions and the "left" FHL. The FHLs difference of the Samples 3, 5, 7 is defined only by the relative thickness of these layers and their *Tcomp.*, this ultimately defines the FHL of the film as a whole. Thus, the "left" FHL of the film/substrate layer, where the magnetization is due to the octahedral sublattice, affects significantly the FHL type of the film as a whole.

The Sample 2 (being single-layer one according to the XRD) is characterized as magneto-inhomogeneous according its FHL. At the film/substrate interface, the FHLs are "right", the Ga^{3+} and Al^{3+} content is less than 1 at./f.u. With increasing h, the FHL shape becomes complex, because the top layer with high concentration of Ga^{3+} and Al^{3+} and the "left" FHL is growing. Thus, the "right" FHL of transient film/substrate layer, where the magnetization is due to the tetrahedral sublattice, also influences significantly the resulting FHL appearance of the film as a whole: it

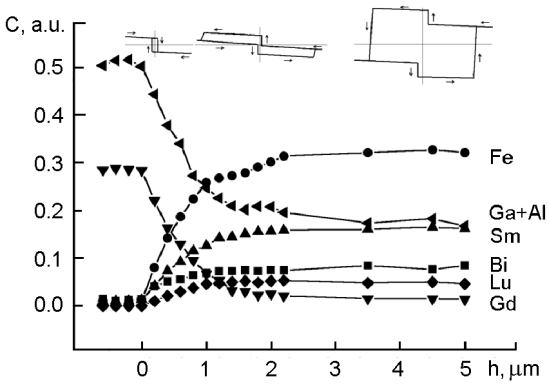

Fig. 3. Concentration depth profile and FHLs of the sample No. 5.

contains lateral hysteresis loops of the film/substrate layer.

The coercive force H_c of the studied films varied in a wide range. Fig. 4 shows the dependence of $H_c(h)$ along the wedge for the Samples 2–5 and 7 at $T = 22°C$. In the Sample 2, H_c changes only slightly from the substrate to $h = 0.8$ μm and increases at $h > 0.8$ μm (Fig. 4a). In the Sample 3, H_c has minimum value at the sample surface (100 Oe) and increases almost 6 times when approaching the substrate (Fig. 4b). In the Samples 4 and 5, $H_c(h)$ dependences are *N*-shaped (Fig. 4c, d). The maximum value $H_c = 2170$ Oe in the Sample 4 is attained at $h \sim 0.9$ μm (Fig. 4c, curve *1*); in the Sample 5, the maximum value $H_c = 4500$ Oe corresponds to $h \sim 2$ μm (Fig. 4d). In the Sample 7, H_c increases with increasing h (Fig. 4e).

It is known that coercive force is maximum near $T_{comp.}$ [11]. Therefore, to explain the $H_c(h)$ behavior, it is important to know $T_{comp.}$. So, in the Sample 2, all FHLs along the wedge are "right", the measurement temperature exceeds $T_{comp.}$ considerably. In the Sample 3, all FHLs along the wedge are "left", the measurement temperature being below $T_{comp.}$, so $T_{comp.}$ has no effect on the results of H_c measurements for these samples. In the Sample 4, the measurement temperature is near $T_{comp.}$ of the layer 2 and this is most likely the cause of *N*-shaped $H_c(h)$ dependence for this sample. Indeed, $H_c(h)$ measurements at $T = 38°C > T_{comp.}$ show that $H_c \approx 200$ Oe along the wedge except for $h = 1.7$ μm, where $H_c = 300$ Oe (Fig. 4c, curve *2*).

Thus, the anomalous dependences $H_c(h)$ in the studied films are due to the proximity of the measurement temperature to $T_{comp.}$ for any layer. In its turn, this is defined by the chemical composition of each

film layer. For example, in Samples 4, 5, 7, on the layer with a high Ga^{3+} concentration (and, respectively, high $T_{comp.}$ and "left" FHL), another layer grows with a lower Ga^{3+} concentration (and, respectively, lower $T_{comp.}$ and "right" FHL), while for Sample 3, the situation is inverse. $T_{comp.}$ of transient layer between these two layers is close t the measurement temperature, and this causes a corresponding H_c increase with increasing h.

The magnetic nature of the $H_c(h)$ anomalies is further evidenced by the investigations of the film surface morphology. Fig. 5 shows the surface photographs of the Sample 4 and GGG-substrate prior to and after various types of surface processing. The H_c values at 22°C are presented, too. The as-grown film surface shows the so-called faceted structure which is then removed by mechanical polishing. After 2 h of ion etching, the butt-end traces of the revealed columnar structure with different faceting become apparent in small number, the size is 1–3 μm in diameter. When $h < 2$ μm, these traces, "uncovered" by the ion beam, cover the entire microscope view field. When approaching the substrate (region 3), their size is increased to 6 μm in diameter. The traces of the columns constituting the film structure are observed at the substrate surface even after a prolonged (6 h) etching. The surface of the clean substrate after ion etching does not show such a pattern. Similar images were obtained for the other studied films. However, the different $H_c(h)$ dependences near the interfaces of the samples as well as analysis of the $H_c(h)$ temperature dependence indicate that the presence of the columnar structure is not essential in defining the nature of the $H_c(h)$ dependence. The ion etching did not affect significantly the $H_c(h)$, too, due to low ion energy. The $H_c(h)$ dependence is defined to a greater extent by $T_{comp.}$ changes in the transient layers of film-substrate interface due to Ga^{3+} and Al^{3+} concentration changes at the crystallization front of the growing film.

4. Conclusion

The magnetic properties of the Bi-substituted iron garnet film / GGG substrate interface are defined by the concentration gradient of the garnet-constituting elements along its thickness. In particular, the observed $H_c(h)$ dependences for different films result from the Ga^{3+} and Al^{3+} ion concentration profile variations. The complex shapes of magneto-optical hysteresis loops

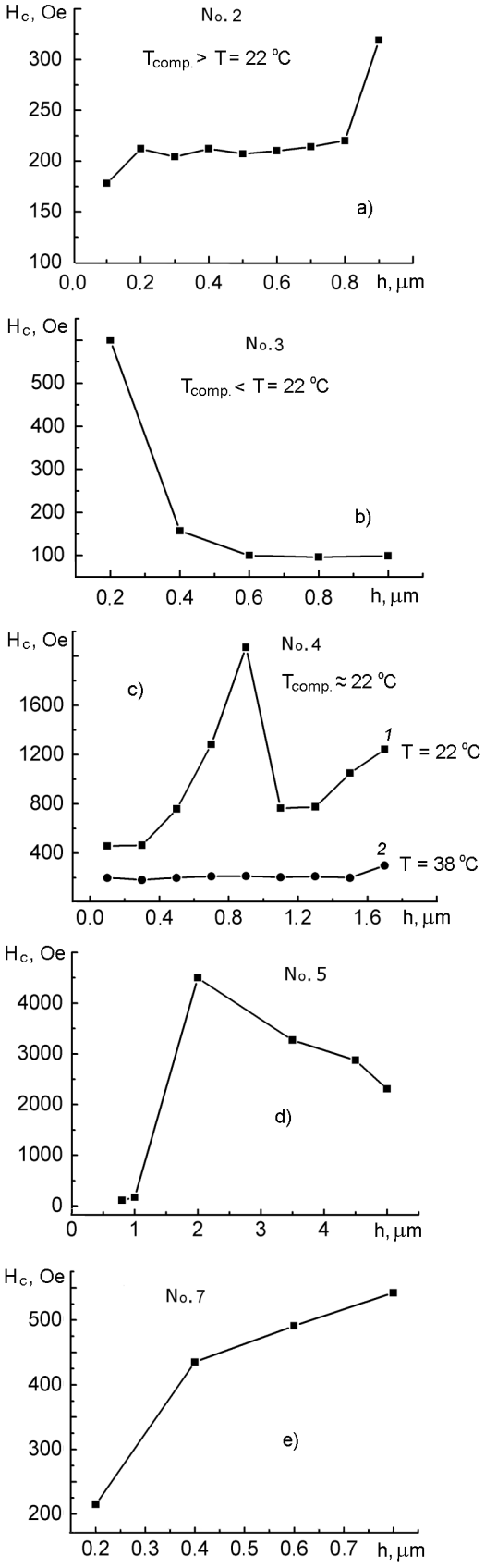

Fig. 4. Thickness dependences of H_c for samples No. 2–5, 7.

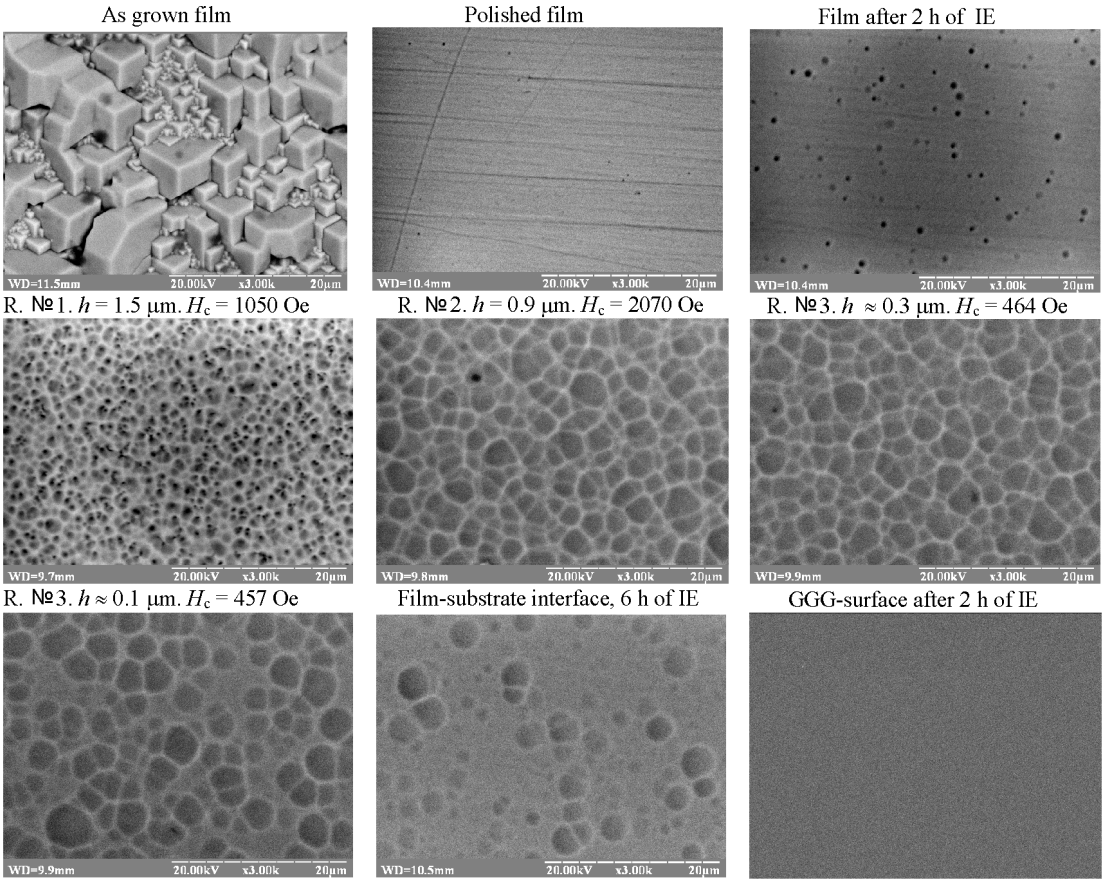

Fig. 5. Photos of surfaces of as-grown,polished and different time (hours) ion etched (IE) films №4 and GGG-surface after 2 h of IE.

and, consequently, the magnetic properties of micrometer thickness films may be defined by the properties of their film/substrate interfaces. In Bi-substituted iron garnet films, the effect of the sublattice magnetic moment "turnover" near the compensation temperature is observed, accompanied by subsequent temperature magnetic hysteresis.

References

1. W.Tolksdorf, G.Bartels, H.J.Tolle, *J. Cryst. Growth*, **52**, 722, (1981).
2. N.A.Groshenko, A.M.Prokhorov, V.V.Randoshkin et al., *Fiz. Tverd. Tela*, **27**, 1712 (1985).
3. N.A.Groshenko, V.V.Randoshkin, A.N.Shaposhnikov et al., *Zh. Tekhn. Fiz.*, **56**, 935 (1986).
4. A.S.Kamzin, Yu.N.Maltsev, *Fiz. Tverd. Tela*, **39**, 1248 (1997).
5. A.S.Kamzin, Yu.N.Maltsev, *Fiz. Tverd. Tela*, **39**, 1410 (1997).
6. U.S. Patent 7,133,189 B2 (2006).
7. A.N.Shaposhnikov, A.R.Prokopov, V.N.Berzhansky et al., in: Memoir of Tavrida Nat. Univ. Ser. Phys., Simferopol, 21 (60), No.1, 153 (2008) [in Russian].
8. V.V.Randoshkin, A.Ya.Chervonenkis, Applied Magnetooptics, Energoatomizdat, Moscow (1990) [in Russian].
9. G.I.Zhuravlev, Chemistry and Technology of Ferrites, Khimia, Leningrad (1970) [in Russian].
10. K.P.Belov, A.K.Zvezdin, A.M.Kadomtseva, Orientation Transitions in Rare-Earth Magnetics, Nauka, Moscow (1979) [in Russian].
11. K.P.Belov, Ferrites in Strong Magnetic Fields, Nauka, Moscow (1972) [in Russian].

Властивості інтерфейсу плівок вісмутвмісного ферит-гранату/підкладка ГГГ

О.М.Шапошников, В.Н.Бержанський, О.Т.Мілюкова, А.В.Каравайников, А.Р.Прокопов

Досліджено концентраційні залежності гранатооутворюючих елементів, магнітні властивості та морфологію поверхні інтерфейсу Bi-вмісних монокристалічних плівок ферит-гранатів складу $(BiSmLu)_3(FeGaAl)_5O_{12}$ / підкладка ГГГ орієнтації (111). Показано, що магнітні властивості та складні форми магнітооптичних петель гістерезису досліджених плівок можуть визначатися властивостями інтерфейсу плівка/підкладка. У деяких плівках поблизу температури компенсації виявлено ефект "перевертання" магнітного моменту підграток, який супроводжується температурним магнітним гістерезисом.